Nanoscale films of δ-Mn on W{001}

2001 J. Phys.: Condens. Matter 13 1805

(http://iopscience.iop.org/0953-8984/13/9/303)

INSTITUTE OF PHYSICS PUBLISHING JOURNAL OF PHYSICS: CONDENSED MATTER

J. Phys.: Condens. Matter **13** (2001) 1805–1810 www.iop.org/Journals/cm PII: S0953-8984(01)16259-4

Nanoscale films of δ-Mn on W{001}

Y Tian and F Jona

Department of Materials Science and Engineering, State University of New York, Stony Brook, NY 11794-2275, USA

Received 10 August 2000, in final form 18 January 2001

Abstract

Ultrathin films of Mn grow pseudomorphically on a W{001} substrate up to 15 or 16 Å. A quantitative low-energy electron diffraction analysis finds the structure of these films to be body-centred tetragonal with the parameters $a = 3.1652$ Å (imposed by the W{001} substrate) and $c = 2.84 \pm 0.06$ Å, and the first interlayer spacing expanded by 0.13 ± 0.03 Å. Identification of the equilibrium phase is made possible by the epitaxial Bain path of antiferromagnetic Mn (as calculated by Qiu, Marcus and Ma), which shows that the structure of these Mn films grown on W{001} is a strained state of the δ-Mn phase.

1. Introduction

Many experiments have been carried out [1–6] in order to try to stabilize at room temperature the δ-phase of Mn, a phase which is stable only between 1133 and 1244 °C and has a body-centred-cubic (bcc) structure with lattice constant $a = 3.0806$ Å at 1134 °C [7].

The experiments involved either the growth of Fe–Mn [2] and Cr–Mn [3] multilayers, or the epitaxial growth of ultrathin films of Mn on single-crystal substrates of Fe{001} [5], Pd{001} [6] and V{001} [8]. However, the multilayer experiments did not provide convincing evidence that δ-Mn had been stabilized. The epitaxial experiments could not be interpreted unambiguously; a fairly detailed discussion of this problem can be found in reference [8]. We give here only a brief summary.

The problem is that, since the Mn films are pseudomorphic with the substrate on which they have been grown, they are strained to assume a tetragonal structure, and in order to decide from which cubic equilibrium phase they have been strained one needs to do a strain analysis. Such an analysis requires knowledge of the crystallographic parameters and of the elastic constants of all possible equilibrium phases, for which in this case there are only two choices: δ-Mn and γ-Mn. The latter is a face-centred-cubic (fcc) phase stable between 1095 and 1133 °C with lattice constant $a = 3.8624$ Å at 1095 °C. However, the scarcity and uncertainty of the available crystallographic and elastic data prevent a confident choice between δ-Mn and γ-Mn as the equilibrium phase.

An elegant and convenient solution of this problem is now possible that provides information about the equilibrium phase and does not require knowledge of the elastic constants. A recent study of tetragonal Mn [9] found that the antiferromagnetic (AF) state of Mn is lower in energy than the ferromagnetic (FM) and nonmagnetic (NM) states, and a

0953-8984/01/091805+06$30.00

subsequent calculation of Qiu, Marcus and Ma (QMM) [10] produced the epitaxial Bain path (EBP) of AF Mn. The EBP is specified by values of the energy per atom E as a function of the axial ratio c/a between the two tetragonal lattice constants c and a. It gives all states that can be produced by epitaxial isotropic strain in the {001} plane in equilibrium phases of the material, which in this case are γ-Mn and δ-Mn. As mentioned above, at high temperatures the γ-Mn phase is fcc (for which $c/a = \sqrt{2}$) and the δ-Mn phase is bcc (for which $c/a = 1$). At lower temperatures, when either phase is stabilized by epitaxy, the structure of AF Mn becomes tetragonal, and the corresponding values of c/a differ from both $\sqrt{2}$ and 1, respectively, but it is customary to keep referring to the phase with c/a close to $\sqrt{2}$ as the γ-phase and to that with c/a close to 1 as the δ-phase.

The calculations of QMM [10] were done with two different potentials: the local spin-density approximation without relativistic corrections (LSDA-NREL), and the Perdew–Burke–Ernzerhof exchange–correlation potential in a generalized-gradient approximation with relativistic corrections (GGA-REL). A useful aspect of the EBP is a plot of the reduced volume V/V_0 versus c/a, where $V = a^2c/2$ is the volume per atom at each value of c/a, and V_0 is the (theoretical) volume per atom in the ground state, i.e. in the present case γ-Mn. Two such curves, as calculated by QMM [10], are depicted in figure 1, one obtained from the LSDA-NREL calculation (solid curve) and one obtained from the GGA-REL calculation (dashed curve).

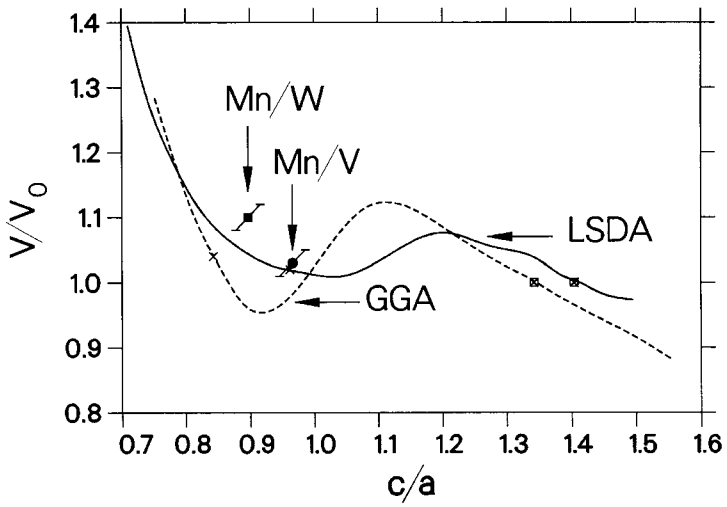

Figure 1. The epitaxial Bain path of antiferromagnetic Mn, after reference [10] (solid: LSDA; dashed: GGA). Crosses and circled crosses mark the δ-Mn and the γ-Mn phases, respectively. The full circle and square mark the experimental results for Mn on V{001} [8] and Mn on W{001} (this work).

The positions of the equilibrium phases on the EBP are indicated with crosses for δ-Mn (at $c/a = 0.843$ for the GGA calculation and $c/a = 0.962$ for the LSDA calculation) and with circled crosses for γ-Mn (at $c/a = 1.342$ for the GGA calculation and $c/a = 1.404$ for the LSDA calculation). In each curve the section contained (approximately) between the minimum and the maximum volume is a region of intrinsically unstable states [11]. An important and useful property of the EBP is that it divides the plane of the plot into three regions: two regions around the corresponding equilibrium phases separated by a region of intrinsically unstable states.

Identification of the equilibrium phase for a film grown epitaxially on a given substrate is easy and unambiguous with the EBP, provided of course that one determines with an appropriate experiment the *actual* lattice parameters a_{exp} and c_{exp} of the film grown. An appropriate experiment is, e.g., a structure determination with quantitative low-energy electron diffraction (QLEED). One then enters on the EBP the experimental point defined by the values of c_{exp}/a_{exp} and of V/V_0 (with $V = a_{exp}^2 c_{exp}/2$, and $V_0 =$ *experimental* equilibrium volume of γ-Mn). If the experimental point falls in the region of the δ-Mn (or γ-Mn) equilibrium phase, then the film structure is a strained state of the δ-Mn (or γ-Mn) equilibrium phase. Thus, QMM have shown [10] that the Mn film grown epitaxially on V{001} is strained δ-Mn, while the one grown on Pd{001} is strained γ-Mn. The Mn film grown on Fe{001} falls in the unstable region of the EBP with both potentials, so no choice of its equilibrium state can be made.

The availability of the EBP for AF Mn makes it now possible to evaluate the findings of a recent study of Mn films grown epitaxially on a W{001} substrate. We report below the results of such a study. We describe the experiment in section 2; the structure analysis in section 3; and the conclusions in section 4.

2. Experiment

The W substrate, a {001} platelet approximately $8 \times 9 \times 0.5$ mm^3, was appropriately mounted on a sample holder in an experimental chamber capable of reaching pressures of 1×10^{-10} Torr or lower. Auger electron spectroscopy (AES) revealed that the major impurity on and in the W sample was C. After about seven hours of Ar-ion bombardment (5×10^{-5} Torr of Ar, 1 μA current, 375 eV ion energy) the ratio R of AES intensities $R =$ C(272 eV)/W(169 eV) was reduced to 6%, but increased to 36% after annealing to 700 °C, and further reduced to 5% after an additional 13 h of Ar bombardment. The sample was then subjected to 8 h of Ar bombardment at 800 °C, and then to 6 h of the same at room temperature, after which treatment no C peak was detectable above the noise in the AES scans (i.e. less than $R = 2\%$). However, after about 1 h with the sample at room temperature, a weak c(2×2) LEED pattern became observable. For this reason, the deposition of Mn on the substrate was initiated shortly after the last annealing treatment, while the sample was cooling, but still approximately at 150 °C.

Manganese was deposited onto the W{001} substrate from a source consisting of small chunks of the material in a tungsten basket that was heated electrically. The deposition rate varied between 0.5 and 0.8 Å min^{-1}. The Mn coverage was monitored by means of the ratio between the Mn AES line at 589 eV and the W line at 169 eV (the procedure is described, e.g., in reference [12]). The LEED pattern was observed and $I(V)$ curves were collected after approximately each incremental 2 or 3 Å; the pattern always remained 1×1. The $I(V)$ curves began to change from those of the W{001} substrate after a coverage of 2 to 2.5 Å, continued to change with increasing Mn deposition and became stable after about 10 or 11 Å, now wholly different from those of clean W{001}. Manganese films thicker than about 18 or 20 Å produced no LEED pattern, indicative of the disappearance of the long-range order that existed in thinner films.

The sequence just described was repeated three times. After each growth sequence, the sample was recleaned with Ar bombardments: 12 h at room temperature followed by 7 h at 800 °C, followed by 1 h with the sample cooling to room temperature, after which the sample was annealed to about 1500 °C for 3 min. The $I(V)$ data used in the intensity analysis described below were collected from a Mn film 14 Å thick: they are the 10, 11, 20 and 21 curves from 60 to 400 eV. The LEED pattern was notably better (sharper spots, lower background) than the norm for most ultrathin pseudomorphic films.

3. Structure analysis

The calculations of the LEED beam intensities produced by the Mn film were made with the full-dynamical program CHANGE [13] including 89 beams and eight phase shifts up to 400 eV. The Mn potential needed for the corresponding phase shifts was obtained from the collection of Moruzzi *et al* [14]. The real part of the inner potential was initially chosen at 10 eV (adjustable during the analysis—the final value was 10 ± 3 eV), the imaginary part was 4 eV and the root mean square amplitude of thermal vibrations $(\langle u^2 \rangle)^{1/2} = 0.07$ Å.

The calculations assumed that the Mn film was semi-infinite (an assumption justified by the fact that the $I(V)$ curves were stable, i.e. independent of the film thickness) with an in-plane lattice constant of 3.1652 Å imposed by the pseudomorphism with the W{001} substrate. The bulk interlayer spacing d_{bulk} was varied initially from 0.9 Å to 2.1 Å in steps of 0.2 Å, and later from 1.32 Å to 1.60 Å in steps of 0.02 Å, in each case with the change Δd_{12} of the first interlayer spacing d_{12} varied from -0.20 to +0.20 Å in steps of 0.02 Å.

The agreement between calculated and observed $I(V)$ spectra was gauged both visually and by R-factor analysis with three R-factors: R_{VHT} [15], r_{ZJ} [16] and R_P [17]. The best agreement was found (both visually and by R-factor) for a bulk interlayer spacing of $d_{bulk} = 1.42 \pm 0.03$ Å and a first interlayer spacing of $d_{12} = d_{bulk} + \Delta d_{12}$ with $\Delta d_{12} = 0.13 \pm 0.03$ Å, with $R_{VHT} = 0.24$, $r_{ZJ} = 0.09$ and $R_P = 0.36$. With these values of d_{bulk} and d_{12}, tests were made for the second interlayer spacing d_{23}, but all three R-factors indicated preference for unchanged d_{23}, i.e. $d_{23} = d_{bulk}$.

Figure 2 depicts the 10, 11, 20 and 21 $I(V)$ curves, both experimental (solid) and theoretical (dotted), showing a very good fit for a strained pseudomorphic film.

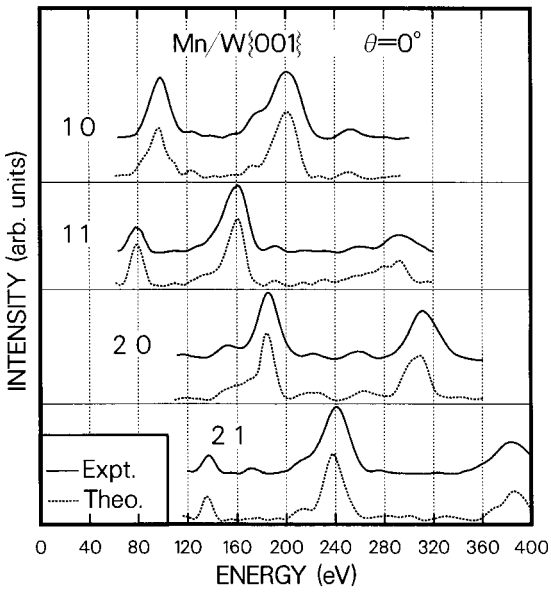

Figure 2. Experimental (solid, from a 14 Å film) and theoretical (dotted, for a semi-infinite crystal) LEED $I(V)$ spectra for Mn on W{001} at normal incidence of the primary beam.

4. Conclusions

The experiment and the QLEED analysis show that the actual structure of the Mn film is bct with $a = 3.1652$ Å (imposed by the W{001} substrate) and $c = 2 \times 1.42 = 2.84$ Å. The question is, what is the equilibrium phase?

The answer to this question can be found on the EBP of AF Mn depicted in figure 1. From the experimental result we calculate $c/a = 0.897$ and the volume per atom $V = 14.23$ Å^3. We normalize this volume by dividing it by the experimental value [18] of the volume of the γ-Mn phase $V_0 = 12.94$ Å^3, so that $V/V_0 = 1.10$. We then plot the point on the EBP.

Figure 1 shows that this point (the full square labelled Mn/W) lies on the left of the instability region for *both* the LSDA and the GGA curves, i.e. in the region pertaining to the δ-Mn phase. The error bars do not reach the EBP curves, and therefore the fit to either curve is not as good as for the Mn/V experimental point (which is mildly surprising, because both the quality of the LEED pattern and the agreement between the $I(V)$ curves is at least as good for Mn/W{001} as for Mn/V{001}, if not better), but there can be no doubt that the Mn films grown on W{001} are strained states of the δ-Mn phase.

The usefulness of the EBP in determining the equilibrium phase of pseudomorphic films is therefore confirmed by the present result. We summarize in table 1 the assignments made with the help of the EBP to the Mn films grown on Pd{001}, Fe{001}, V{001} and W{001}. The table lists the misfits of the selected substrates to the a-parameters of γ-Mn and δ-Mn, and shows that the misfits are often fair predictors of the outcome of an epitaxial experiment, especially with regard to the GGA values: for Mn/V and Mn/W the smallest misfits point to the δ-Mn phase, as confirmed by the EBP, while for Mn/Pd the large misfit to δ-Mn and the small one to γ-Mn clearly favour the latter. This observation is useful, because in the search for the most suitable substrate for a given epitaxial experiment aimed at stabilizing a metastable phase, the only guide is the misfit of the selected substrate to the lattice constant of the metastable phase found by the EBP.

Table 1. Epitaxial growth of Mn films on four substrates: Pd{001}, Fe{001}, V{001} and W{001}, with lattice constants a_{sub} in Å [7]. The table lists the misfits of each substrate to γ-Mn (experimental data from reference [17]) and δ-Mn (theoretical data from reference [10]) with the following lattice parameters (lengths in Å): for γ-Mn (experiment): $a = 2.684$, $c = 3.592$, $c/a = 1.338$; for δ-Mn (theory): LDA: $a = 2.787$, $c = 2.680$, $c/a = 0.962$; GGA: $a = 3.067$, $c = 2.585$, $c/a = 0.843$. The values of c/a listed below are experimental data from the references cited. The 'Equilibrium phase' column lists the equilibrium phases of the Mn films grown as determined from the EBPs published in reference [10].

	Misfit to			Mn film	
Substrate (a_{sub} (Å))	γ-Mn	δ-Mn (LDA)	δ-Mn (GGA)	c/a	Equilibrium phase
Pd (2.751[a])	+2.5%	−1.3%	−10.3%	1.247[b]	γ-Mn
Fe (2.866[a])	+6.8%	+2.8%	−6.6%	1.126[c]	Uncertain
V (3.023[a])	+12.6%	+8.5%	−1.4%	0.966[d]	δ-Mn
W (3.165[a])	+17.9%	+13.6%	+3.2%	0.897[e]	δ-Mn

[a] Reference [7].
[b] Reference [6].
[c] Reference [5].
[d] Reference [8].
[e] This work.

Acknowledgments

We are indebted to the National Science Foundation for partial support of the work described in this paper with Grant DMR-9806651. We also thank Shen-Li Qiu for kindly providing the data for the EBPs plotted in figure 1.

References

[1] Heinrich B, Arrott A S, Cochran J F, Liu C and Myrtle K 1986 *J. Vac. Sci. Technol.* A **4** 1376
Heinrich B, Arrott A S, Liu C and Purcell S T 1987 *J. Vac. Sci. Technol.* A **5** 1935
[2] Pohl J, Malang E U, Scheele B, Köhler J, Lux-Steiner M Ch and Bucher E 1994 *J. Vac. Sci. Technol.* B **12** 3202
[3] Pohl J, Malang E U, Köhler J and Bucher E 1995 *J. Vac. Sci. Technol.* A **13** 295
[4] Pohl J, Christensen M J, Huljic D, Köhler J, Malang E U, Albrecht M and Bucher E 1997 *J. Appl. Phys.* **81** 169
[5] Kim S K, Tian Y, Montesano M, Jona F and Marcus P M 1996 *Phys. Rev.* B **54** 5081
[6] Tian D, Wu S C, Jona F and Marcus P M 1989 *Solid State Commun.* **70** 199
[7] Pearson W B 1958 *A Handbook of Lattice Spacings and Structures of Metals and Alloys* (Oxford: Pergamon)
Pearson W B 1967 *A Handbook of Lattice Spacings and Structures of Metals and Alloys* (Oxford: Pergamon)
[8] Tian Y, Jona F and Marcus P M 1999 *Phys. Rev.* B **59** 12 647
[9] Qiu S L and Marcus P M 1999 *Phys. Rev.* B **60** 14 533
[10] Qiu S L, Marcus P M and Ma H 2000 *Phys. Rev.* B **62** 3292
[11] Marcus P M and Alippi P 1998 *Phys. Rev.* B **57** 1971
[12] Kim S K, Jona F and Marcus P M 1996 *J. Phys.: Condens. Matter* **8** 25 (equation (1))
[13] Jepsen D W 1980 *Phys. Rev.* B **22** 5701
Jepsen D W 1980 *Phys. Rev.* B **22** 814
[14] Moruzzi V L, Janak J F and Williams A R 1978 *Calculated Electronic Properties of Metals* (New York: Pergamon)
[15] Van Hove M A, Tong S Y and Elconin M H 1977 *Surf. Sci.* **64** 85
[16] Zanazzi E and Jona F 1977 *Surf. Sci.* **62** 61
[17] Pendry J B 1980 *J. Phys. C: Solid State Phys.* **13** 937
[18] Endoh Y and Ishikawa Y 1971 *J. Phys. Soc. Japan* **30** 1614